Neutron diffraction study of low-temperature magnetic phase diagram of an isosceles-triangular-lattice Ising antiferromagnet $CoNb_2O_6$

S. Kobayashi,[1,*] S. Mitsuda,[2] S. Hosaka,[2] H. Tamatsukuri,[2] T. Nakajima,[2] H. Koorikawa,[2] K. Prokeš,[3] and K. Kiefer[3]
[1]*Department of Materials Science and Engineering, Faculty of Engineering, Iwate University, Ueda 4-3-5, Morioka 020-8551, Japan*
[2]*Department of Physics, Faculty of Science, Tokyo University of Science, Shinjuku-ku, Tokyo 162-8601, Japan*
[3]*Helmholtz-Zentrum Berlin für Materialien und Energie, Hahn-Meitner Platz 1, Berlin 14109, Germany*
(Received 13 June 2016; published 27 October 2016)

A low-temperature magnetic phase diagram under magnetic fields along the orthorhombic a axis of an isosceles-triangular-lattice antiferromagnet $CoNb_2O_6$ was investigated through single-crystal neutron diffraction measurements made at temperatures down to $T = 0.5$ K. We produced a phase diagram that consists of three magnetically ordered phases, i.e., the antiferromagnetic (AF), the incommensurate sinusoidal magnetic (IC), and the induced ferromagnetic (IFM) phases, which were characterized by the propagation wave vectors $\mathbf{Q} = (0\ \frac{1}{2}\ 0)$, $(0\ q\ 0)$, and $(0\ 0\ 0)$, respectively. We found that a field-induced ferrimagnetic phase with $\mathbf{Q} = (0\ \frac{1}{4}\ 0)$ that had been observed by previous neutron diffraction studies down to $T = 1.8$ K [H. Weitzel *et al.*, Phys. Rev. B **62**, 12146 (2000)] does not exist as a single equilibrium phase, but rather it always coexists with the other ordered phases near the triple point where the AF, IC, and IFM phases meet. We also found that the relaxation time of the system becomes extremely long below $T = 0.6$ K in comparison with our observation time; this was considered to possibly be the reason for magnetization plateaus appearing at $T = 0.5$ K. These plateaus have a half-saturation magnetization, from which another field-induced state was inferred in previous magnetization measurements [J. Phys. Soc. Jpn. **63**, 2706 (1994)].

DOI: 10.1103/PhysRevB.94.134427

I. INTRODUCTION

Geometrically frustrated triangular-lattice antiferromagnets have attracted considerable interest because of their diverse phase transitions and critical phenomena, which originate from the macroscopic degeneracy of their ground state [1,2]. When a triangular geometrical frustration is partially released, for example, because of an orthorhombic distortion, the nearest-neighbor antiferromagnetic interaction of a triangular lattice is split into two inequivalent antiferromagnetic interactions, as a result the degeneracy of the ground state is partially lifted and magnetic features reflecting the ratio of antiferromagnetic interactions may appear. Frustrated isosceles triangular lattices, however, have proven to be worth investigating further; far from being just an intermediate case between frustrated triangular-lattice antiferromagnets and unfrustrated magnets, they also exhibited the potential for unusual magnetic features that are absent in both antiferromagnets and unfrustrated magnets [3–6].

A columbite niobate $CoNb_2O_6$ is one such example of an isosceles-triangular-lattice antiferromagnet [7–14]. It has a crystal structure with a space group of $Pbcn$ (No. 60), where staggered chains of CoO_6 or NbO_6 octahedra run along the c axis and are formed by sharing two edges, as shown in Fig. 1(a). Co^{2+} and Nb^{5+} ions form separate two-dimensional sheets, which stack along the a axis as Co-Nb-Nb-Co. The lattice parameters for the orthorhombic unit cell at $T = 1.5$ K are $a = 14.17$ Å, $b = 5.71$ Å, and $c = 5.04$ Å [8]. The allowed nuclear reflection conditions are $k = 2n$ for $0\ k\ l$, $l = 2n$ for $h\ 0\ l$, $h + k = 2n$ for $h\ k\ 0$, $h = 2n$ for $h\ 0\ 0$, $k = 2n$ for $0\ k\ 0$, and $l = 2n$ for $0\ 0\ l$; those in the $(0\ k\ l)$ zone are schematically shown in Fig. 1(b).

As shown in Fig. 1(a), magnetic Co^{2+} ions form quasi-one-dimensional (quasi-1D) ferromagnetic zigzag chains along the c axis and form an isosceles triangular lattice in the a-b plane. In a zero field, $CoNb_2O_6$ exhibits successive magnetic phase transitions from the paramagnetic (PM) phase to the incommensurate sinusoidal magnetic (IC) phase through a temperature-dependent propagation wave vector $\mathbf{Q}_{IC} = (0\ q\ 0)$ at $T_1 \sim 3.0$ K, before moving to the noncollinear antiferromagnetic (AF) phase, with $\mathbf{Q}_{AF} = (0\ \frac{1}{2}\ 0)$ at $T_2 \sim 1.9$ K; the AF structure is shown in Fig. 1(c). Here, the Co^{2+} spins are confined to two different easy axes in the a-c plane with a canting angle of θ_0 (=31°) from the c axis, which originates from two crystallographically nonequivalent octahedral CoO_6 sites. Extensive investigations into the magnetic fields along the c axis have revealed various magnetic features reflecting spin frustration on the isosceles triangular lattice, such as magnetic structure-dependent spin correlations along the a axis [8], anisotropic and extremely slow domain-growth kinetics [9,11], and a rich magnetic-field (H) versus temperature (T) phase diagram that consists of AF, IC, induced ferromagnetic (IFM) phases, field-induced ferrimagnetic (FR) phase with $\mathbf{Q} = (0\ \frac{1}{3}\ 0)$, higher-field ferrimagnetic (HHFR) phase with $\mathbf{Q} = (0\ \frac{1}{2}\ 0)$, and low-temperature higher-field ferrimagnetic (LHFR) phase with $\mathbf{Q} = (0\ \frac{1}{3}\ 0)$ [10,13–15]. These features have been qualitatively explained by an isosceles-triangular-lattice Ising model that has a nearest-neighbor antiferromagnetic interaction J_1, along with a next-nearest one J_2, with $\gamma = J_1/J_2$ being 1.33; this is not far from the 1.0 of the triangular lattice [16].

When a magnetic field is applied along the direction in the a-c plane at a finite angle to the c axis, interesting magnetic features are expected because of the two different easy axes. Weitzel *et al.* performed neutron diffraction measurements down to $T = 1.7$ K under magnetic fields along various

*koba@iwate-u.ac.jp

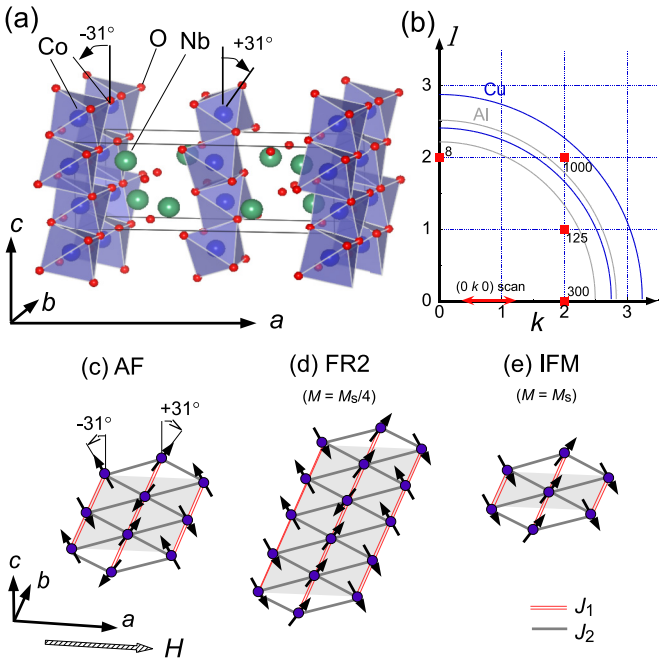

FIG. 1. (a) Crystal structure of $CoNb_2O_6$. Co^{2+} ions occupy the 4(*c*) site in the *Pbcn*: (0 y_0 $\frac{1}{4}$), (0 $-y_0$ $\frac{3}{4}$), ($\frac{1}{2}$ $\frac{1}{2}$ + y_0 $\frac{1}{4}$), and ($\frac{1}{2}$ $\frac{1}{2}$ − y_0 $\frac{3}{4}$) with $y_0 = 0.165$ [13]. (b) Schematic drawing of the reciprocal lattice in the (0 *k l*) zone for $k \geqslant 0$ and $l \geqslant 0$. The nuclear Bragg points are shown by the squares; the numbers shown close to the symbols are the calculated neutron intensities for when a (0 2 2) intensity is normalized to 1000. The red arrows represent the location of the neutron diffraction (0 *k* 0) reciprocal lattice scan. The gray and blue lines denote the positions of the nuclear Bragg peaks coming from Al and Cu, respectively, which were used to fix a sample or cryomagnet. The magnetic structures of (c) AF, (d) FR2, and (e) IFM phases are shown under applied fields along the *a* axis. Magnetic Co^{2+} ions form an isosceles triangular lattice in the *a*-*b* plane with interchain antiferromagnetic exchange interactions J_1 and J_2. The arrows represent Co^{2+} spins. All the spins were confined to easy axes on the *a*-*c* plane canted from the *c* axis. The shaded area corresponds to a magnetic unit cell.

directions in the *a*-*c* plane, and they proposed an *H*-*T* magnetic phase diagram that included several field-induced ferrimagnetic phases with different propagation vectors, whose stability depends on the angle of magnetic field to the *c* axis [14]. Magnetic phases that make up the *H*-*T* phase diagram are the same as those for field along the *c* axis, for angles up to ∼45°; however, another ferrimagnetic phase with $\mathbf{Q} = (0\ \frac{1}{4}\ 0)$ shows up between the two FR and HHFR phases for angles greater than ∼45°; hereafter, we will call this the ferrimagnetic phase FR2. By increasing the angle to ∼60°, the FR phase completely disappears and for applied fields along the *a* axis only the FR2 phase appears as a field-induced ferrimagnetic phase. These magnetic phase diagrams were qualitatively reproduced by a mean-field numerical approach similar to that done by Boehm *et al.* [17], using a full Hamiltonian, complete with competing exchange interactions on an isosceles triangular lattice, a crystal field, and dipolar-dipolar interactions [14].

Although there is a deep understanding of the magnetic features under applied fields in $CoNb_2O_6$ [7,8,10,13,14], two unresolved issues remain for applied fields along the *a* axis. (1) For neutron diffraction measurements down to $T = 1.7$ K, Weitzel *et al.* proposed a $H_{\|a}$-T magnetic phase diagram that consists of the AF, IC, FR2, and IFM phases, where the FR2 phase appears in the intermediate magnetic-field and temperature ranges of roughly $H = 700$–1200 Oe and $T = 1.7$–2.5 K [Fig. 5(b)] [14,18]. With regards to magnetic reflections obtained under applied fields forming an angle of ∼45° to the *c* axis, Weitzel *et al.* proposed a magnetic structure of the FR2 and IFM phases; these are shown in Figs. 1(d) and 1(e), respectively. Although the proposed FR2 structure has a saturation magnetization of $M_s/4$ along the *a* axis, magnetization along the *a* axis monotonically increases with the field in the intermediate magnetic-field range and a magnetization plateau corresponding to the appearance of the FR2 phase is not observed [7,14]. This implies that the FR2 state is metastable and does not exist as a thermodynamic equilibrium phase for applied fields along the *a* axis. Actually, there is a large discrepancy in the calculated $H_{\|a}$-T phase diagram that assumes the full Hamiltonian; a phase transition from the AF to IFM phase occurs directly, and the field-induced FR2 phase does not actually appear in the calculated $H_{\|a}$-T phase diagram. (2) Hanawa *et al.* surveyed a $H_{\|a}$-T magnetic phase diagram using magnetization and specific-heat measurements down to $T = 0.5$ K [7]. They found that an IFM phase is field induced under low fields of ∼1.5 kOe at all measured temperatures below T_1. In particular, at the lowest measured temperature of 0.5 K, a magnetization plateau with a half-saturation magnetization $M_s/2$ can be seen; this implies that there is an intermediate field-induced phase between the AF and IFM phases. The details of this intermediate phase and its relation with the higher-temperature FR2 phase remains unclear.

In this study, we performed low-temperature neutron diffraction and magnetization measurements down to $T = 0.5$ K on a single crystal of $CoNb_2O_6$ under a magnetic field applied along the *a* axis. We did this in order to investigate how a field-induced ferrimagnetic phase characterized by $\mathbf{Q}_{FR2} = (0\ \frac{1}{4}\ 0)$, as suggested by Weitzel *et al.*, is extended in the lower-temperature region in the $H_{\|a}$-T phase diagram, and to understand how it connects with the half-magnetization plateau at $T = 0.5$ K that had been reported by Hanawa *et al.* The low-temperature $H_{\|a}$-T magnetic phase diagram of $CoNb_2O_6$ was also constructed.

II. EXPERIMENT

A single crystal with dimensions of $5 \times 5 \times 10$ mm^3 was grown through the flux method [19]. The crystal has previously been used in earlier neutron diffraction studies [8,10]. Neutron diffraction measurements were performed with a two-axis diffractometer E4, which is housed at the Helmholtz-Zentrum Berlin (HZB). A pyrolytic graphite filter was used to eliminate second-order contamination, and incident neutrons with a wavelength of 2.44 Å were used. A vertical external field along the *a* axis up to 2 kOe, and a temperature down to 0.5 K, were provided by a 5-T superconducting cryomagnet (VM-3) with a helium-3 insert. The sample was mounted so as to access

the (0 k l) scattering plane in the reciprocal lattice. Reciprocal lattice scans were performed with increasing magnetic field after the sample had been cooled down to 0.5 K before being heated to a measuring temperature in the zero field.

The dc magnetic measurements down to $T = 0.5$ K were performed with a commercial superconducting quantum interference device (SQUID) magnetometer (Quantum Design MPMS-XL) equipped with a helium-3 refrigerator (ihelium3). A magnetic field along the a axis up to 2 kOe was applied and the magnetization along the a axis was measured as a function of the magnetic field in the hysteresis mode.

III. RESULTS AND DISCUSSION

A. Neutron diffraction measurements

Figures 2(a)–2(d) show the (0 k 0) reciprocal-lattice scans, which were taken by increasing the magnetic field at several temperatures below T_1. At the lowest temperature of 0.5 K, an AF peak with $q = \frac{1}{2}$ appeared in the zero field and started to diminish at around $H = 500$ Oe as the magnetic field increased; this was associated with the appearance of the (0 1 0) peak in the IFM phase as shown in Fig. 2(a). As the magnetic field further increased, the IFM peak developed and the field-induced AF-IFM phase transition occurred at around $H = 700$ Oe. In order to investigate the possibility of another magnetic state(s) appearing during the AF-IFM phase transition, we performed a wide omega scan by rotating the sample 180° as along with a wide (0 k 1) reciprocal-lattice scan with $k = -0.1$–2.1 at $H = 750$ Oe. Since a two-dimensional detector had been employed in our experiments, a wide range of reciprocal-lattice space including that of an out-of-scattering plane space ($|h| <\sim 0.7$) could also be surveyed. No detectable magnetic reflections were observed within an experimental accuracy, however, except for those of the AF and IFM phases. This ensured that magnetic states with a propagation vector of (0 q 0), (0 q $\frac{1}{2}$), or (q_x q 0) with $q = 0$–1.0 and $q_x = 0$–1.0 were not realized during the AF-IFM transition. As the magnetic field increased further, the AF peak persisted up to a high magnetic field of 1.5 kOe as shown in the inset in Fig. 2(a). The magnetic phase transition at $T = 0.5$ K is a direct AF-IFM phase transition and no field-induced intermediate phase was observed between the AF and IFM phases.

At $T = 1.85$ K, an AF peak appeared in zero field and a field-induced AF-IC phase transition occurred at a low applied field of ∼150 Oe along with the coexistence of both the AF and IC peaks as shown in Fig. 2(b). As the magnetic field increased, the IC peaks located at (0 q 0) and (0 1–q 0) with $q \sim 0.48$ gradually shifted towards the (0 0 0) and (0 1 0) IFM peak positions, respectively. At the same time, the IC peaks became strongly broadened and their peak intensities largely decreased; this was associated with the evolution of the (0 1 0) IFM peak. At around $H = 800$ Oe, a broad magnetic peak centered at $k \sim 0.75$ was observed beside a broad IC peak at $k \sim 0.7$ as shown in the inset in Fig. 2(b). Since the width of the magnetic peak at $k \sim 0.75$ is comparable to that of the IC peak, the magnetic peak at $k \sim 0.75$ may actually be composed of many magnetic peaks with different propagation wave numbers that are equal and close to the $q = \frac{1}{4}$ of the FR2 state. In other words, at around $H = 800$ Oe, the magnetic domains of the FR2 state with $q = \frac{1}{4}$ and the IC states with

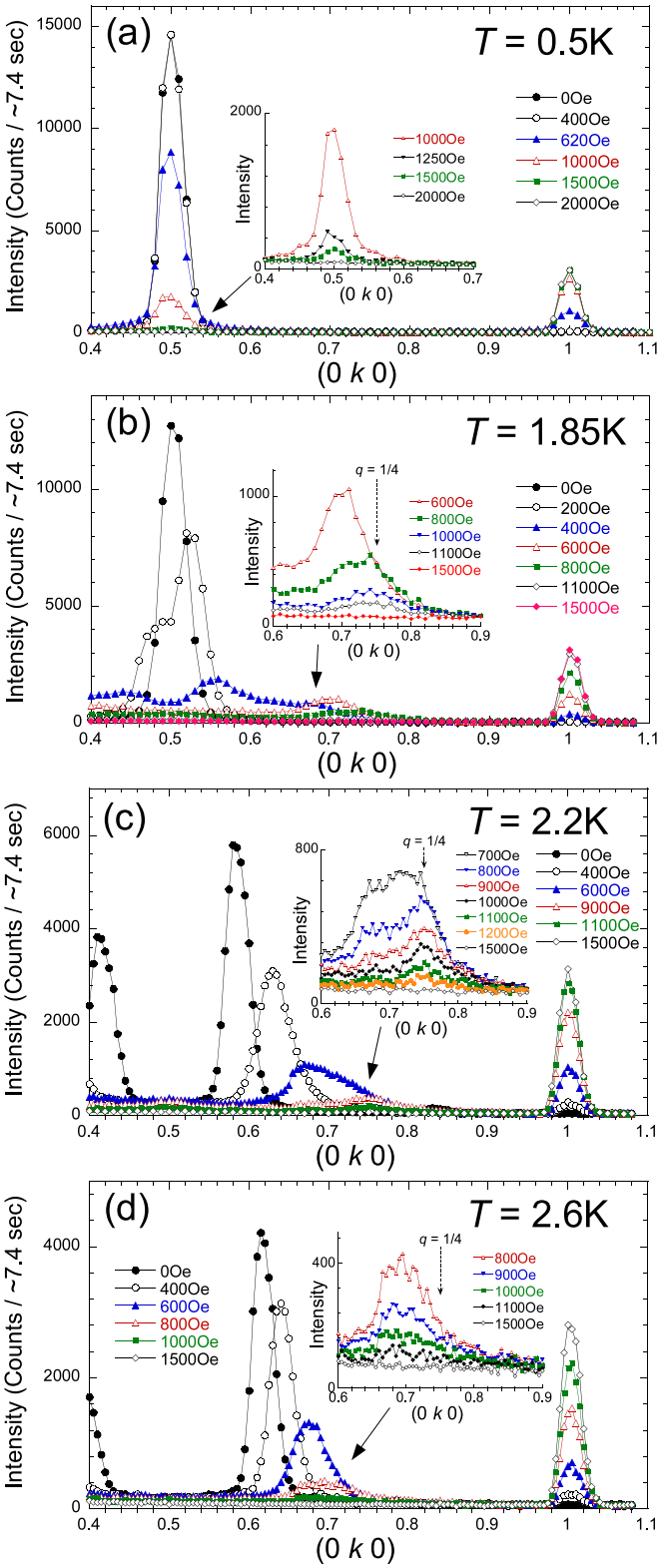

FIG. 2. The magnetic-field dependence of the representative neutron diffraction (0 k 0) reciprocal-lattice scans at (a) $T = 0.5$ K, (b) $T = 1.85$ K, (c) $T = 2.2$ K, and (d) $T = 2.6$ K. The insets show their enlargement in the medium field range.

q close to $\frac{1}{4}$ are also present in the crystal along with the IC domains with $q \sim 0.3$.

Hereafter, we will call this broad magnetic peak centered at around the FR2 peak position the FR2 peak for the sake of simplicity. By increasing the magnetic field, the intensity of both the IC and FR2 peaks diminished and the IC peak disappeared around $H = 1000$ Oe; the broad FR2 peak nevertheless persisted up to the slightly higher field of 1100 Oe above which the IFM ordering was almost achieved. A similar field dependence of the FR2 peak was observed at $T = 2.2$ K, which is just above T_2 as shown in Fig. 2(c), where the IC ordering became stabilized in the zero field. On the other hand, at high temperatures above ∼2.5 K, a simple field-induced IC-IFM phase transition took place as the magnetic field increased and no FR2 peak was observed, as shown in Fig. 2(d). These observations strongly indicate that the FR2 state with $q = \frac{1}{4}$, as originally observed by Weitzel *et al.* [14], does not appear as a single equilibrium phase, but rather it always coexists with the IC and/or IFM phases.

In Figs. 3(a)–3(h), the magnetic-field dependence of q and the integrated intensities obtained from these (0 k 0) scans are summarized. For magnetic fields where both the IC and FR2 peaks overlapped, data were obtained by least-squares fits assuming double Gaussian profiles. Note again that the data for the FR2 peak may have originated from many magnetic peaks that had different q values equal or close to $\frac{1}{4}$. As shown in Figs. 3(f) and 3(g), the integrated intensity of the FR2 peak maximized in the intermediate magnetic fields of 800–900 Oe and temperatures of ∼2.2 K, but the intensity of the FR2 peak was much smaller than that of the IC and/or IFM peaks.

Next, in order to investigate how the FR2 peak extended into the low-temperature region, we performed (0 k 0) reciprocal-lattice scans at a fixed magnetic field of 900 Oe while cooling from $T = 2.2$ K. As shown in Fig. 4, at $H = 900$ Oe and $T = 2.2$ K, several broad magnetic peaks were observed in addition to the sharp (0 1 0) IFM peak; a (0 1–q 0) FR2 peak with $q = \frac{1}{4}$ located at $k = \frac{3}{4}$, its 2q and 1–2q both located at $k = \frac{1}{2}$, and a small (0 1–q 0) IC peak with $q \sim 0.32$ located at $k \sim 0.68$. As the temperature decreased, the FR2 peak at $k = \frac{3}{4}$ and the IC peak suddenly started to diminish just below $T = 1.85$ K, and they completely disappear at $T = 1.5$ K. This accompanied a large increase in the (0 $\frac{1}{2}$ 0) peak intensity as well as a slight decrease in the (0 1 0) one. These observations suggest that most of the magnetic domains, which contribute to broad FR2 and IC peaks, were changed into AF ordered regions at low temperatures below $T \sim 1.5$ K. Furthermore, below $T \sim 1.5$ K a small and broad magnetic peak around $k = 0.9$, as well as a strong broadening of the AF peak, were observed; this may reflect a difficulty in the magnetic moment rearranging at low temperatures so as to form a long-range AF order.

In Fig. 5, the H-T magnetic phase diagram obtained from the present neutron diffraction study is summarized. A critical field was defined as the midpoint between the magnetic fields of the higher- and lower-field phases at which their integrated intensities became half of their maximum value. The phase diagram consists of the AF, IC, and IFM phases. The coexistence regions for the AF and IFM orders, and for the IC and IFM orders, extend over a wide H-T area, i.e., approximately 1 kOe along the field axis. In addition, the FR2 state, which may be an assembly of magnetic states with different wave numbers that are equal or close to $\frac{1}{4}$, always coexists with the other ordered state, and it appears near the triple point where the AF, IC, and IFM phases meet. This may reflect the presence of many quasidegenerate ground states with q from 0 to $\frac{1}{2}$ near the triple point.

The H-T magnetic phase diagram determined by this study is largely different from that proposed by Weitzel *et al.* shown in Fig. 5(b). In their phase diagram, the FR2 phase is represented as a stable magnetic phase, although the detail on how the phase boundary of the FR2 phase was determined is not given [14]; furthermore, no data about the neutron diffraction patterns under the magnetic fields along the a axis are shown. Nevertheless, we cannot rule out the possibility of a sample dependence in the volume fraction of the FR2 state, which is created by a sample imperfection like point defects (vacancy, impurity atom for Co site) or surface effect which may stabilize the FR2 state.

As discussed in our previous study [8], a sample imperfection and surface effect can modify the stability of the magnetic phases. For instance, in the AF phase with $\mathbf{Q}_{\mathrm{AF}} = (0\ \frac{1}{2}\ 0)$, we observed a small volume fraction of another antiferromagnetic (AF2) phase characterized by $\mathbf{Q}_{\mathrm{AF2}} = (\frac{1}{2}\ \frac{1}{2}\ 0)$, which coexisted with the AF phase. The volume fraction of the AF2 phase was 0.4%–2% for single-crystal samples, and it was sample dependent. The AF2 structure had a magnetic unit cell doubling as the chemical unit cell along both the a and b axes, while the AF structure was only along the b axis, as shown in Fig. 1(c). In the AF phase, the exchange interaction J_2 along the a axis was effectively canceled out by the up-down-up-down spin arrangement along the b axis, and further neighbor exchange interactions along the a axis were considered to play an important role in the magnetic correlations along the a axis. As a result, we inferred that the appearance of the AF2 phase was due to an inhomogeneity in the further neighbor exchange interactions that originated from either a sample imperfection or a surface effect. A recent study on polycrystalline $CoNb_2O_6$ revealed that there indeed was a large volume fraction of the AF2 phase [20]. Moreover, another recent study, this time on $Co_{1-x}Mg_xNb_2O_6$ under a magnetic field along the c axis, demonstrated that adding only 0.4% of nonmagnetic Mg ions at the Co site would make both the AF and the field-induced FR phases unstable, and as a result a H-T region of the IC phase would extend towards the lower-temperature region as well as a higher magnetic field [21]. These observations strongly indicate that sample imperfections or surface effects can locally and very weakly modify the exchange interactions that occur on isosceles triangular lattices in $CoNb_2O_6$, lift the degeneracy of ground states, and lead to the appearance of other magnetic states as a new ground state. Near the triple point where the AF, IC, and IFM phases meet, the magnetic states with q from 0 to $\frac{1}{2}$ are quasidegenerated, and as a result it is highly possible that a sample dependence of the volume fraction of the FR2 state resulting from sample imperfections or surface effects leads to the discrepancy in the two H-T magnetic phase diagrams of Figs. 5(a) and 5(b). It should be noted that the FR2 peak observed at $H = 900$ Oe, taken after cooling from a higher temperature to 2.2 K in the zero field, is also strongly broadened and its volume fraction is almost the same as that obtained after heating from $T = 0.5$ K; this

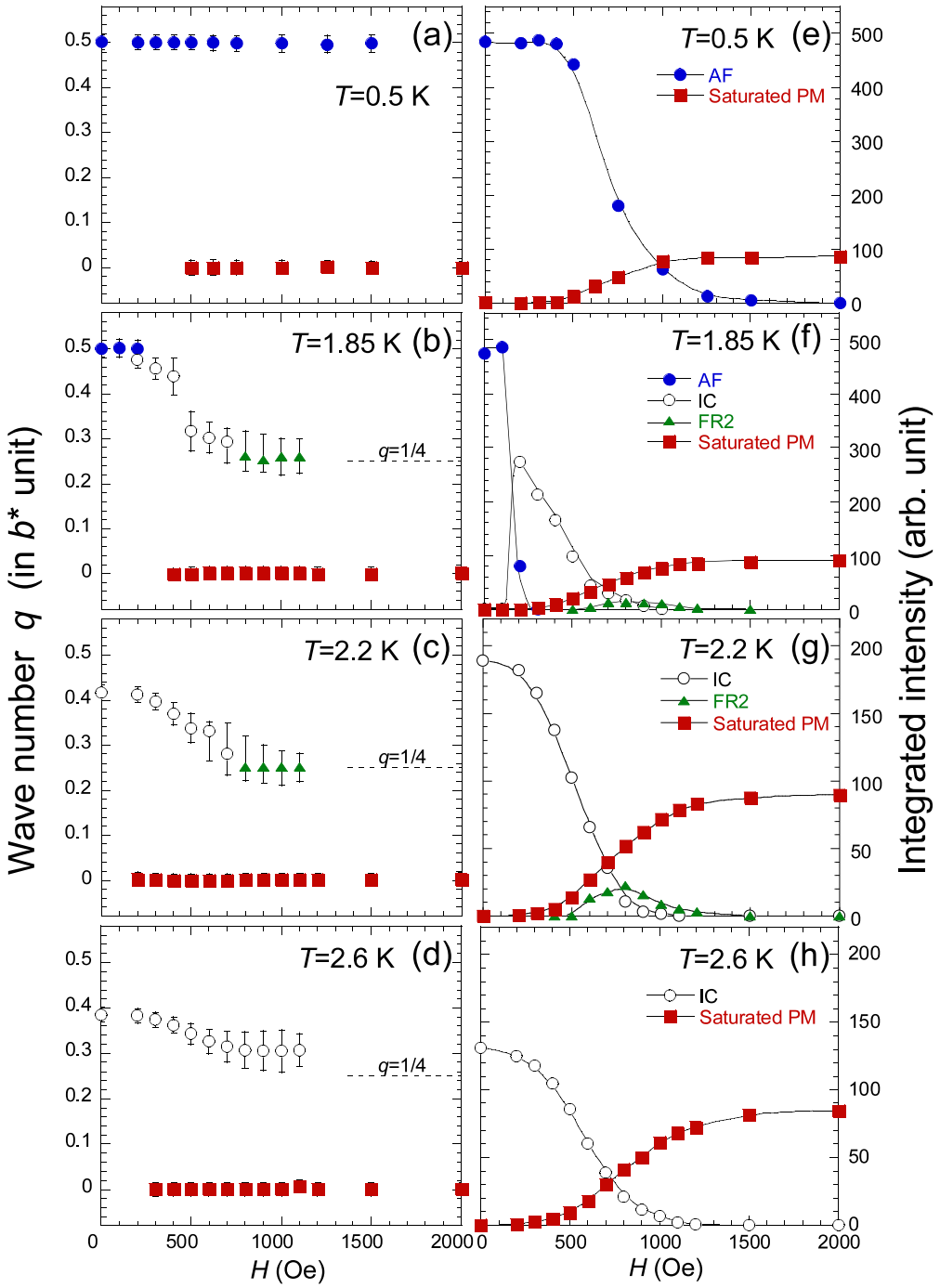

FIG. 3. The magnetic-field dependence of the propagation wave number q in the b^* direction [(a)–(d)] at several temperatures below T_1. The closed circles, open circles, triangles, and squares represent data from the AF, IC, FR2, and IFM peaks, respectively. For magnetic fields at $T = 1.85$ and 2.2 K, where the IC and FR2 peaks both coexist, q was taken from the peak position. In order to show how the IC and FR2 peaks anomalously broadened, the full width at half maximum of a magnetic peak is given as the vertical bars in (a)–(d). The magnetic-field dependence of the integrated intensities of the (0 1–q 0) peak [(e)–(h)] at several temperatures below T_1. The solid lines through the data act as visual guides.

means that the absence of the long-range FR2 ordering in the present sample is not due to the temperature history.

Next, in order to investigate the detailed magnetic structures under the magnetic fields along the a axis, we surveyed integrated intensities of several magnetic Bragg points for both IFM and FR2 states. The magnetic structural analysis was carried out because the proposed magnetic structures in Figs. 1(c) and 1(d) were based on neutron diffraction measurements for applied fields forming at an angle of ∼45° to the c axis, and not for applied fields along the a axis. First, we will show the results for the IFM phase. Integrated intensities were collected by θ–2θ scans for several magnetic Bragg points in the (0 k l) zone. Figure 6(a) shows the relation between the observed integrated intensities I_{obs} and calculated

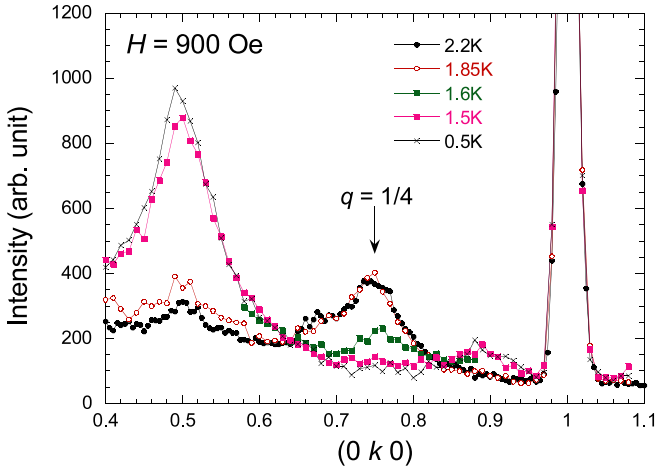

FIG. 4. Temperature dependence of the neutron diffraction profile of the (0 k 0) scans, taken at $H = 900$ Oe.

ones I_{cal} by assuming the magnetic structure of Fig. 1(e). Here, the magnetic Bragg peaks that are masked by a large nuclear Bragg peak or contaminated by Al and Cu [see Fig. 1(b)] were not included in Fig. 6(a). The good linear relationship confirms the magnetic structure of Fig. 1(e) in the IFM phase, and is consistent with previous studies [7,13,14].

Next, we pay attention to the magnetic structure of the FR2 state. Figure 6(b) shows a I_{obs} versus I_{cal} curve, with the FR2 structure from Fig. 1(d) assumed. Here, the integrated intensities of the magnetic Bragg peaks, at (0 k 0) and (0 k 1) with k up to 2.25, expected from the FR2 structure with $\mathbf{Q}_{FR2} = (0\ \frac{1}{4}\ 0)$ were collected at $H = 900$ Oe and $T = 2.2$ K. The intensities for the k = integer were eliminated by the significant contribution of the IFM phase. One can see that there is a rough proportional relationship between I_{obs} and I_{cal}, but data for the (0 $\frac{1}{2}$ 0) reflection exhibits a large deviation, and so the detailed magnetic structure was not identified. We also tested other magnetic structural models with a magnetic unit cell along the b axis of four chemical systems that are energetically probable within our isosceles-triangular-lattice Ising model [8], but a large deviation from the (0 $\frac{1}{2}$ 0) point still remains, and the proportional relationship between I_{obs} versus I_{cal} could not be improved upon. Since the magnetic peaks were strongly broadened and the instrumental resolution was finite, the observed integrated intensities taken from the θ–2θ scans always included intensities due to the IC states that had a q close to $\frac{1}{4}$; this may be another reason for the poor proportionality in the I_{obs}-I_{cal} curve for the FR2 state.

B. Magnetic measurements

Previous magnetization measurements that had been by Hanawa *et al.* reported on the appearance of magnetization plateaus for $M \sim M_s/2$ at $T = 0.5$ K in the intermediate field range between the AF and IFM phases [7]. This indicates that another field-induced intermediate magnetic state appeared. However, in the present neutron diffraction study, the corresponding magnetic state was not confirmed at $T = 0.5$ K. In order to elucidate the reason why such half-magnetization plateaus appeared in that earlier study, we carried out detailed dc magnetization measurements with a commercial SQUID

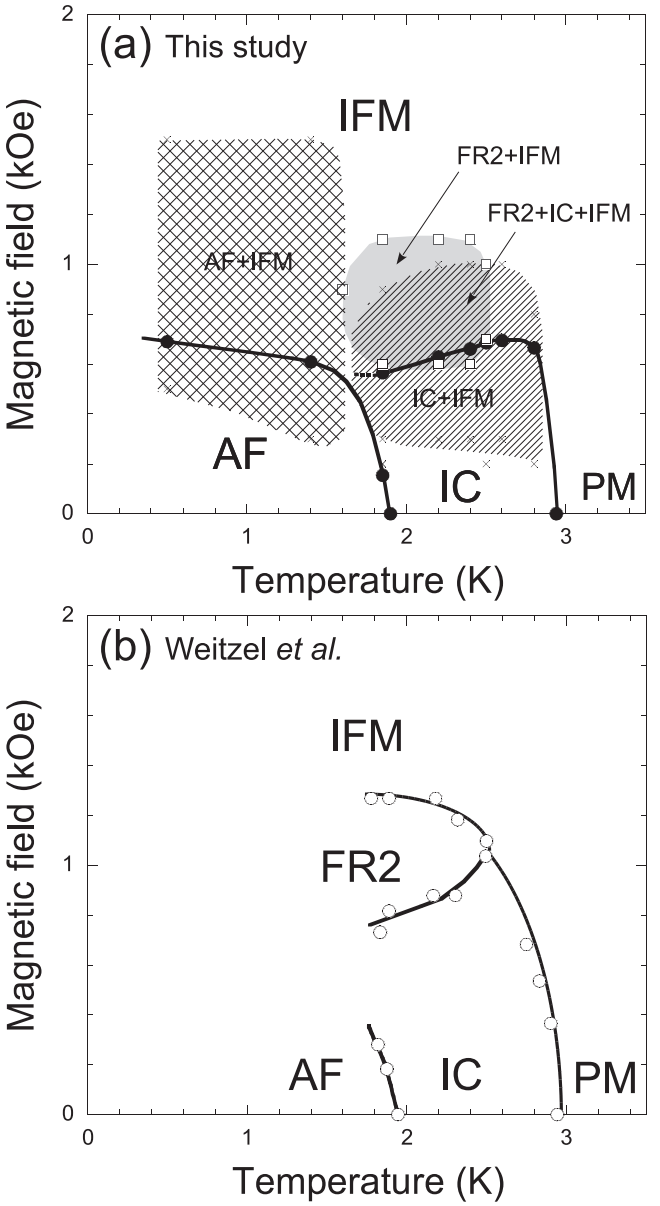

FIG. 5. (a) The H-T phase diagram for the applied field along the a axis, as determined by this study. The solid circles at the finite field represent the critical fields that were determined from neutron integrated intensities, whereas those in the zero field are taken from Ref. [8]. The cross-hatched and hatched areas represent the H-T region where the AF and IC phases coexist with the IFM one, respectively. The boundaries of the coexistence regions were determined by using the data points shown by the crosses. The H-T region where the FR2 peak was observed is shown by the shaded area, and is surrounded by square symbols. The shaded area is the coexistence region for the FR2 and IFM states, while the region where the shaded and hatched areas overlap implies the coexistence region for the FR2, IC, and IFM states. (b) The H-T phase diagram for the applied field along the a axis, as proposed by Weitzel *et al.*, was reproduced using data given in Ref. [14]. This diagram was made so that an easily comparison could be made with this study.

magnetometer. Note that Hanawa *et al.* measured the M-H curves by using an induction method that continuously made a sweeping magnetic field with a rate of ~67 Oe/s, whereas

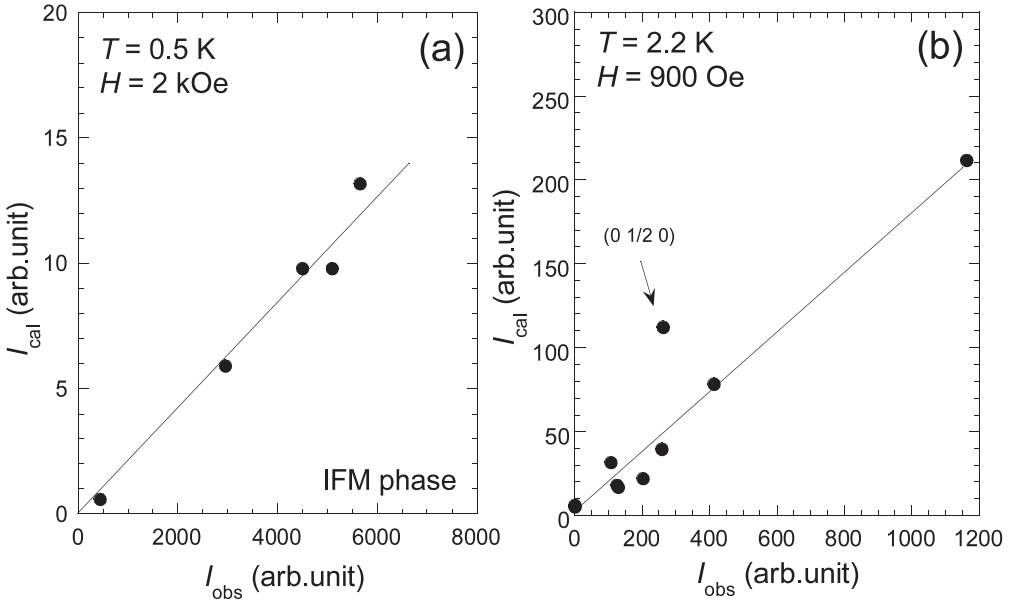

FIG. 6. The observed and calculated integrated intensities, taken at (a) $H = 2$ kOe and $T = 0.5$ K for the IFM phase, and (b) $H = 900$ Oe and $T = 2.2$ K for the coexistence phase of the IFM and FR2 phases.

a magnetic field was varied step by step with an interval of 50 Oe with a similar rate of ∼40 Oe/s in the present dc measurements. Figure 7 shows magnetization as a function of the magnetic field along the a axis, taken at $T = 0.5$ K. The M-H curves were measured with a field cycle of $0 \rightarrow 2000 \rightarrow 0$ Oe. Two independent measurements, i.e., the first and second trials, were done in order to see if the data could be reproduced. As the magnetic field increased, a sudden increase in the magnetization occurred at $H \sim 600$ Oe for the first trial,

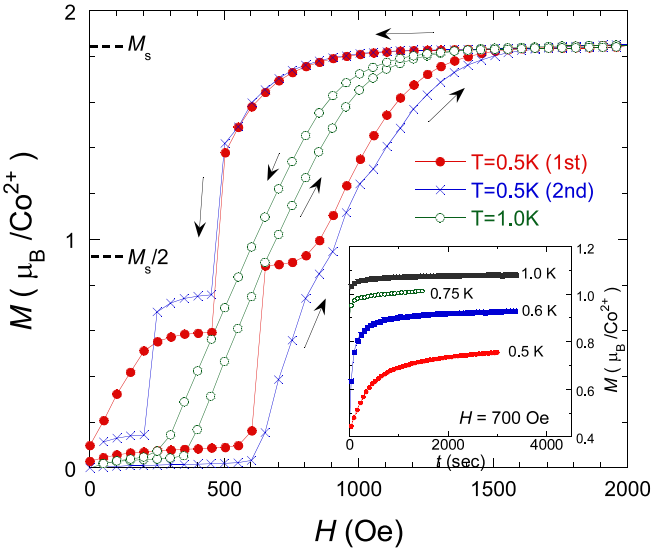

FIG. 7. (a) Magnetization as a function of the magnetic field along the a axis, taken at $T = 0.5$ K. The first and second trials were independently performed with the same experimental setup. For comparison, the data taken at $T = 1.0$ K are also given. The inset shows the time dependence of magnetization at $H = 700$ Oe after a sudden field change from the zero field at several temperatures at and below $T = 1.0$ K.

whereas for the second trial a clear magnetization jump was not observed. On the descending branch of M-H curves, a magnetization jump was found to occur at $H \sim 500$ Oe for both cases, but another magnetization jump occurred at $H \sim 200$ Oe for the second trial only. Just after the magnetization jump, the magnetization reached almost the same value as that achieved at $T = 1.0$ K, and then it showed magnetization plateaus; $M \sim 0.5M_s$ for the increasing field and $0.44M_s$, $0.33M_s$, $0.08M_s$ for the decreasing field. These observations indicate that the magnetization plateaus that implied an intermediate state at $T = 0.5$ K are not reproducible.

As revealed in our previous neutron diffraction study for applied fields along the c axis [10], the relaxation time of this system is extremely long at temperatures below ∼0.6 K in comparison to our observation time. Therefore, it is possible that the energetically unfavorable ferromagnetic quasi-1D chains that formed along the c axis were frozen, which led to the appearance of magnetization plateaus with various magnetization values. In order to check the relaxation behavior for applied fields along the a axis, we measured the time dependence of the magnetization at $H = 700$ Oe after a sudden field change from $H = 0$ Oe at several temperatures between 0.5 and 1.0 K as shown in the inset in Fig. 7. At $T = 1.0$ K, the magnetization just after reaching $H = 700$ Oe already had a high value, almost being the same as that of Fig. 7, and was weakly dependent on time; this indicated that the system went into an equilibrium state after only a short observation time. The magnetization just after the field change became lower as the temperature decreased, and it exhibited an extremely long time relaxation below $T = 0.6$ K. Even after 3 ks, the magnetization at $T = 0.5$ K was approximately 70% of the value obtained at $T = 1.0$ K. These results suggest that the relaxation time becomes extremely long below $T \sim 0.6$ K for applied fields along the a axis as well.

At $T = 0.5$ K, the magnetization jump frequently occurred as the magnetic field increased or decreased, and it was accompanied by a reversal of many ferromagnetic quasi-1D

chains running along the c axis. Just after the reversals, the magnetization reached nearly the same value as it had had at $T = 1.0$ K. Therefore, the system would be in a near-equilibrium state at a given magnetic field just after the magnetization jump. However, the system may not follow a subsequent change in the external field, due to an extremely long time relaxation being responsible for the appearance of the magnetization plateaus at $T = 0.5$ K, as shown in Fig. 7. Note that, although a magnetization increase accompanied an increase in the PM peak intensity, a sudden change in the PM peak intensity due to the magnetization jump was not observed in the magnetic -field dependence of the integrated intensity at $T = 0.5$ K, shown in Fig. 3(e). The time taken for the neutron data collection, from $H = 0$ to the maximum field of 2 kOe, is at least 4 h; this is much longer than ∼30 min needed for the M-H data collection, and it implies it was likely the system reached a near-equilibrium state during the neutron data collection. This long measurement time, combined with the low number of data points collected for the neutron data as opposed to the magnetization data, may be a possible reason as to why a sudden change in the IFM peak intensity did not occur as magnetic field increased.

IV. SUMMARY

A low-temperature magnetic phase diagram under a magnetic-field run along the a axis of an isosceles-triangular-lattice antiferromagnet made of $CoNb_2O_6$ was investigated through neutron diffraction measurements made at temperatures going down to $T = 0.5$ K. We found that a field-induced FR2 phase characterized by the propagation wave vector $\mathbf{Q}_{FR2} = (0\ \frac{1}{4}\ 0)$ does not exist as a thermodynamic equilibrium phase. In our H-T phase diagram, only the AF, IC, and IFM phases appear, while the FR2 state always appears as a coexistence state with the IFM and IC phases (or IFM phase) at an intermediate temperature and magnetic field near the triple point where the AF, IC, and IFM phases meet. The dc magnetization measurements were carried out at temperatures down to $T = 0.5$ K, and we found that the field-induced intermediate state with half-magnetization, which had been inferred from the magnetization plateaus at $T = 0.5$ K, was found to originate from the long relaxation time of the system, which became extremely slow below $T \sim 0.6$ K.

ACKNOWLEDGMENTS

This work was supported by a Grant-in-Aid for Scientific Research (C) (Grants No. 23540424 and No. 26400369) from JSPS, Japan. We thank HZB for the allocation of neutron beamtime. The neutron diffraction experiments at HZB were performed according to Proposal No. PHY-01-3176. The crystal structure figure was drawn using the VESTA software [22].

[1] H. T. Diep, *Frustrated Spin Systems* (World Scientific, Singapore, 2004).
[2] M. F. Collins and O. A. Petrenko, Can. J. Phys. **75**, 605 (1997).
[3] J. Stephenson, J. Math. Phys. **11**, 420 (1970).
[4] J. Stephenson, Can. J. Phys. **48**, 2118 (1970).
[5] J. Doczi-Reger and P. C. Hemmer, Phys. A (Amsterdam) **108**, 531 (1981).
[6] S. B. Lee, R. K. Kaul, and L. Balents, Nat. Phys. **6**, 702 (2010).
[7] T. Hanawa, K. Shinkawa, M. Ishikawa, K. Miyatani, K. Saito, and K. Kohn, J. Phys. Soc. Jpn. **63**, 2706 (1994).
[8] S. Kobayashi, S. Mitsuda, M. Ishikawa, K. Miyatani, and K. Kohn, Phys. Rev. B **60**, 3331 (1999).
[9] S. Kobayashi, S. Mitsuda, T. Jogetsu, J. Miyamoto, H. Katagiri, and K. Kohn, Phys. Rev. B **60**, R9908 (1999).
[10] S. Kobayashi, S. Mitsuda, and K. Prokes, Phys. Rev. B **63**, 024415 (2000).
[11] S. Kobayashi, H. Okano, T. Jogetsu, J. Miyamoto, and S. Mitsuda, Phys. Rev. B **69**, 144430 (2004).
[12] S. Kobayashi, S. Hosaka, H. Tamatsukuri, T. Nakajima, S. Mitsuda, K. Prokes, and K. Kiefer, Phys. Rev. B **90**, 060412(R) (2014).
[13] C. Heid, H. Weitzel, P. Burlet, M. Bonnet, W. Gonschorek, T. Vogt, J. Norwig, and H. Fuess, J. Magn. Magn. Mater. **151**, 123 (1995).
[14] H. Weitzel, H. Ehrenberg, C. Heid, H. Fuess, and P. Burlet, Phys. Rev. B **62**, 12146 (2000).
[15] The FR and HHFR phases in Ref. [10] correspond to the SF1 and SF2 phases given in Ref. [14], respectively. The LHFR phase appears only at low temperatures below $T \sim 0.6$ K (Ref. [10]) and was not reported in neutron diffraction study down to $T = 1.5$ K of Ref. [14].
[16] In this study, we redefined the $J_2 \cos 2\theta_0$ of our previous study (Ref. [8]) as J_2 for simplicity. Here, the term $\cos 2\theta_0$ originates from the two different easy axes along which the Co spins align.
[17] J. von Boehm and P. Bak, Phys. Rev. Lett. **42**, 122 (1979).
[18] The FR2 and IFM phases correspond to the SF3 and F_a phases given in Ref. [14], respectively.
[19] B. M. Wanklyn, B. J. Garrard, and G. Garton, Mater. Res. Bull. **11**, 1497 (1976).
[20] P. W. C. Sarvezuk, E. J. Kinast, C. V. Colin, M. A. Gusmao, J. B. M. da Cunha, and O. Isnard, J. Appl. Phys. **109**, 07E160 (2011).
[21] T. Nakajima, S. Mitsuda, H. Okano, Y. Inomoto, S. Kobayashi, K. Prokes, S. Gerischer, and P. Smeibidl, J. Phys. Soc. Jpn. **83**, 094723 (2014).
[22] K. Momma and F. Izumi, J. Appl. Crystallogr. **44**, 1272 (2011).